Increased gyrification in Williams syndrome: evidence using 3D MRI methods

J Eric Schmitt BA BS;
Katie Watts;
Stephan Eliez MD, Stanford Psychiatry Neuroimaging Laboratory, Department of Psychiatry and Behavioral Sciences, Stanford University School of Medicine, Stanford;
Ursula Bellugi EdD, Laboratory for Cognitive Neurosciences, The Salk Institute for Biological Studies, LaJolla, CA;
Albert M Galaburda MD, Division of Behavioral Neurology, Beth Israel Deaconess Medical Center, Harvard University School of Medicine, Cambridge, MA;
Allan L Reiss* MD, Stanford Psychiatry Neuroimaging Laboratory, Department of Psychiatry and Behavioral Sciences, Stanford University School of Medicine, Stanford, CA, USA.

**Correspondence to last author at* Department of Psychiatry and Behavioral Sciences, Stanford University School of Medicine, 401 Quarry Road, Stanford, CA 94305-5719, USA.
E-mail: areiss1@leland.stanford.edu

Understanding patterns of gyrification in neurogenetic disorders helps to uncover the neurodevelopmental etiology underlying behavioral phenotypes. This is particularly true in Williams syndrome (WS), a condition caused by de novo deletion of approximately 1 to 2 Mb in the 7q11.23 region. Individuals with WS characteristically possess an unusual dissociation between deficits in visual–spatial ability and relative preservations in language, music, and social drive. A preliminary postmortem study reported anomalous gyri and sulci in individuals with WS. The present study examined gyrification patterns in 17 participants with WS (10 females, 7 males; mean age 28 years 11 months, SD 8 years 6 months) and 17 age- and sex-matched typically developing control participants (mean age 29 years 1 month, SD 8 years 1 month) using new automated techniques in MRI. Significantly increased cortical gyrification was found globally with abnormalities being more marked in the right parietal (p=0.0227), right occipital (p=0.0249), and left frontal (p=0.0086) regions. These results suggest that one or more genes in the 7q11.23 region are involved during the critical period when cortical folding occurs, and may be related to the hypothesized dorsal/ventral dissociation in this condition.

Advances in neurogenetics are steadily increasing existing knowledge on the genetic origins of behavior and cognition. In Williams syndrome (WS), both the genetic cause and the cognitive profile are well characterized. The genetic hallmark of WS is a deletion of approximately 20 contiguous genes on the long arm of chromosome 7 (Korenberg et al. 2000). The deletion is associated with physical characteristics including specific facial features, cardiovascular malformations, failure to thrive in infancy, and neonatal hypercalcemia (Morris et al. 1988, Trauner et al. 1989). The cognitive profile of WS includes relative strengths in verbal expression, face processing, and musical abilities, with weaknesses in spatial cognition and visual–motor abilities (Bellugi et al. 1999, 2000).

Previous neuroimaging studies on WS have revealed a decrease in overall brain volume with relative preservation of cerebellar volume, as well as asymmetric distribution of occipital lobe tissue volume (Reiss et al. 2000). Postmortem observations have shown polymicrogyri and other gyral abnormalities in a small sample of participants with WS, particularly on the dorsal cortical surface (Galaburda and Bellugi 2000). The purpose of our laboratories' research on this disorder is to further the study of neuroanatomy and brain function in WS with the specific goal of strengthening links between genetic/molecular influences and cognitive characteristics.

The aim of this study was to use in vivo brain images collected with MRI to replicate and quantify the postmortem findings of abnormal gyrification as described in Galaburda and Bellugi (2000). To quantify gyral complexity, our laboratories employed the gyrification index (GI), a commonly used ratio of the inner contours of the brain to its outer contours (Zilles et al. 1988). Most early studies of GI examined either postmortem brains (Vogeley et al. 2000), a limited number of brain sections (Kulynych et al. 1997), or they parcellated the brain by hemisphere only (Bartley et al. 1997). The present study measured gyrification patterns by cerebral lobe using high-resolution MRI and advanced image processing methodologies.

Method

PARTICIPANTS

Seventeen participants diagnosed with WS (10 females, 7 males; mean age 28 years 11 months, SD 8 years 6 months, range 19 to 44 years) and 17 healthy, typically developing control participants (mean age 29 years 1 month, SD 8 years 1 month, range 19 to 48 years), individually matched for age and sex, were recruited by the Laboratory for Cognitive Neuroscience at the Salk Institute, CA, USA. The diagnosis of WS was confirmed genetically by fluorescent in situ hybridization (FISH) probes for elastin, a gene consistently found in the critical deletion region associated with WS (Korenberg et al. 2000). All diagnoses were further confirmed using the Williams Syndrome Association's Diagnostic Scoresheet.

The study was approved by the Human Subjects Committees of both Stanford University and the Salk Institute. Each participant and their guardian, as appropriate, gave informed consent for their participation in the study. Some of the individuals with WS had participated in previous studies (Reiss et al. 2000; Schmitt et al. 2001 Forthcoming).

IMAGING

High-resolution MR images of each participant's brain were acquired with a GE-Signa 1.5 T scanner (General Electric, Milwaukee, WI, USA). Sagittal T_1-weighted images were

acquired with a 3D volumetric radio frequency spoiled gradient echo (SPGR) using the following scan parameters: TR=24, TE=5, flip angle=45, NEX=2, matrix size=256 × 192, field of view=24, slice thickness=1.2 mm, 124 slices.

Images were imported into the computer program, 'BrainImage' (Reiss 2000) for reliable, semi-automated removal of non-brain tissue, and then spatially normalized using a Talairach grid (Talairach and Tournoux 1988). This grid is proportional, adjusting to the size and shape of each individual brain. A region of interest (ROI) delineating the lateral ventricles was manually circumscribed, and all included pixels were changed to white (intensity 255 in an 8-bit color table). This procedure was performed in order to prevent the ventricle–brain perimeter from being included as part of the cortical perimeter in subsequent measurements (see below). These procedures have been described elsewhere (Subramaniam et al. 1997). In addition, the posterior fossa was circumscribed and removed using methods based on a previously validated protocol (Aylward and Reiss 1991).

The remaining cerebral tissue was spatially parcellated based on Talairach sectors that divide the cerebrum into its four major lobes for each hemisphere (Subramaniam et al. 1997). In order to localize possible gyrification anomalies, each lobe was measured separately.

Calculation of Gyrification Index

The fundamental concept of the GI has been described elsewhere (Zilles et al. 1988). GI is defined as the ratio of the inner perimeter of the brain (following all contours into the sulcal crevices) divided by the perimeter of the outer surface:

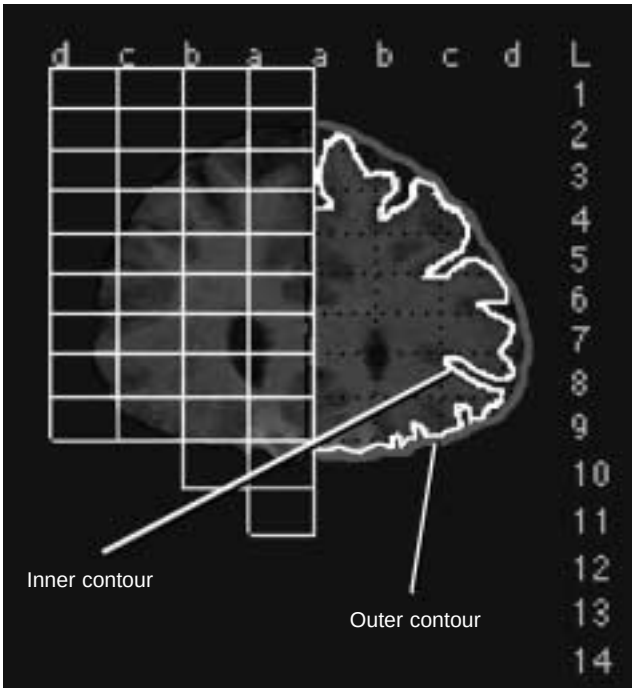

Figure 1: *Example of GI algorithm from image oriented in coronal plane. Inner GI contour is denoted in white, while outer is shown in gray on a slice through frontal lobe. White boxes, numbers, and letters denote Talairach atlas defined sectors encompassing right frontal lobe.*

$$GI = \frac{\text{length of inner contour}}{\text{length of outer contour}}$$

This study used software-based image processing techniques to automate the calculation of GI into a 2.5 dimensional procedure. Briefly, the image was first classified into gray matter, white matter, and CSF using a dual thresholding algorithm that performs discrete tissue segmentation based on a histogram of image intensities (Otsu 1979). The inner contour of the brain could then be defined as the perimeter that included all pixels that had been classified as brain tissue (i.e. voxels that were either gray or white matter). As it excluded all CSF and null voxels, this ROI circumscribed all sulci of the brain, in effect tracing the border between brain tissue and CSF. The perimeter of the ROI was then recorded for input into the GI equation.

To generate the ROI of the outer brain surface, a relaxed convex hull morphological operator was applied with the inner contour ROI as its argument (Lancaster et al. 1999). The algorithm determined the smallest convex polygon that included all points of the original inner contour ROI. In effect, this operator retraced the inner contour ROI but with a virtual 'ball' of a fixed diameter (in this case six voxels, approximately 6 mm in size). Due to the finite size of the ball, the resultant ROI was redefined as the outer surface (i.e. convex hull) of the inner surface ROI (Fig. 1) and the perimeter measured. The above procedure was automatically repeated for each image slice using the following equation:

$$GI = \frac{\sum_{j=1}^{n} P_i t}{\sum_{j=1}^{n} P_o t}$$

where P_i=the inner perimeter for slice j, P_o=the outer perimeter for slice j, t=slice thickness, and n=the number of slices in the image (Fig. 1). The result of each component (e.g. numerator or denominator) of this equation is the surface area of the brain (or lobe), either at its inner or outer contour. Because GI is a ratio, both 't' and the units of perimeter canceled, producing the unitless GI.

DATA ANALYSIS

Data were first examined graphically before formal statistical analysis. Although visual inspection of the variables of interest (right and left frontal, temporal, parietal and occipital lobes) suggested group differences in distribution with more skewing or kurtosis in those with WS, these differences did not reach statistical significance using the Kolmogorov–Smirnov normality test. Therefore, a repeated measures ANOVA was used as an initial statistical procedure. Post hoc non-parametric statistics were then employed on an exploratory basis to investigate potential brain-region specific differences in GI. Specifically, Mann–Whitney *U* tests were used with a two-tailed *p* value of 0.05 set as the significance threshold. Finally, regression analyses were used to determine the effect of age and sex on gyrification for both groups.

Results

Repeated measures ANOVA showed a significant effect for the diagnostic group with those with WS showing increased GI

compared with control participants ($F=5.23$; $p<0.03$). Group by repeated measure (i.e. region) interaction was not significant ($F=1.23$; $p<0.3$). However, post hoc exploratory analyses (Table I) indicated that those with WS had significantly increased gyrification in the right parietal ($p=0.0227$) and right occipital ($p=0.0249$) lobe regions relative to the control group (Fig. 2). Gyrification also was significantly increased in the WS group for the left frontal lobe ($p=0.0086$). There was no significant correlation between GI and age or sex for either group.

Discussion

Results of this study support previous findings of morphological abnormalities of sulcal/gyral anatomy in WS and suggest that these abnormalities may be particularly prominent in the parietal and occipital lobes (Galaburda and Bellugi 2000). The differences might also be related to neurocognitive features associated with WS, for example, impaired visual–spatial skills and behavioral features such as attentional dysfunction, perseveration, and unusual reactions to sound and music (Bellugi et al. 2000). Neuroanatomical studies, both postmortem examinations and imaging studies have also shown differences in this region, particularly in the right hemisphere (Galaburda and Bellugi 2000, Reiss et al. 2000). Differences in the left frontal lobe were somewhat unexpected but may indicate that though volumetric brain differences in WS are predominantly found in the posterior region, cerebral brain morphology may be more globally affected by the genetic deletion.

Understanding these patterns of gyrification is important for determining the neurodevelopmental functions of the deleted genes in WS. Cortical folding is a complex developmental process beginning in the fifth month of pregnancy (Ono et al. 1990, Magnotta et al. 1999). At this stage, when neuronal migration is largely complete, the immature cortex is still relatively smooth; thus subsequent gyrification appears to be driven by localized developmental changes, such as glial proliferation and cell differentiation (Dobbing and Sands 1970). To explain the pattern of enfolding that ensues, Richman and coworkers (1975) propose a mechanical model. In this model, gyrification is driven by stresses created by varying elasticity between the outer stratum and inner stratum of the cerebral cortex leading to differential laminar growth. Other models suggest that gyrification results from the massive expansion of cortical gray matter and the development of interconnecting circuits (Magnotta et al. 1999). The growth rates of different cortical regions should be relatively similar, assuming cortical thickness and cell density do not vary radically throughout the hemisphere (Van Essen and Maunsell 1980).

The exact mechanisms of how cortical folding is disrupted in WS are presently unclear. A possible cause is localized deficiencies in neuron production, which might distort the geometry of the embryonic brain and manifest as an abnormal folding pattern in the adult (Richman 1975, Todd 1982). Morphometric studies of WS suggest that neuronal cell packing density is diminished with a simultaneous increase in glial numbers, possibly indicating a decrease in the total number of neurons as a result of developmental arrest (Galaburda et al. 1994, Galaburda and Bellugi 2000). In addition, Galaburda reports small microvascular gliotic infarcts in the posterior dorsal forebrain in persons with WS, with the parietal lobe particularly affected (Galaburda and Bellugi 2000). As cortical lesions can affect gyral complexity (Rakic 1988), the infarcts seen in WS may contribute to increases in the GI. The exact genetic cause of these neuroanatomic differences in WS is currently unknown.

Several genes deleted in the critical 7q11.28 region in WS are thought to be involved in neurodevelopment, and may contribute to differential patterns of gyrification in this condition.

Table I: Gyrification index (±SD) by cerebral lobe

Lobe	*Williams syndrome*	*Control group*
Left frontal	2.840 (0.403)	2.504 (0.496)
Right frontal	2.648 (0.465)	2.488 (0.455)
Left parietal	2.812 (0.418)	2.613 (0.553)
Right parietal	2.782 (0.441)	2.526 (0.484)
Left temporal	2.579 (0.460)	2.399 (0.567)
Right temporal	2.468 (0.490)	2.334 (0.494)
Left occipital	2.858 (0.480)	2.682 (0.680)
Right occipital	2.982 (0.492)	2.648 (0.511)

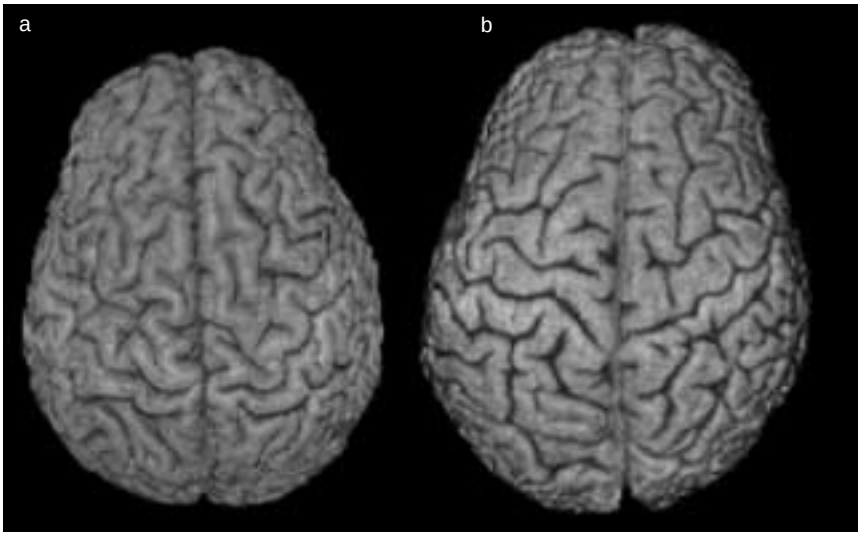

Figure 2: *Differential patterns of gyrification in WS, as demonstrated by rendered surface images of (a) a participant with WS and (b) a typically developing control individual. Note increase in gyral convolutions in WS brain, as opposed to larger gyri and straighter sulci in control. In this example, differences are particularly apparent in parietal region.*

For example, the protein kinase resulting from the gene LIMK1 has been hypothesized to play a role in axonal growth, intracellular signaling, synapse formation, and maintenance in the CNS (Wang et al. 1998). Syntaxin, another protein missing in WS, is thought to be involved in exocytosis of neurotransmitters from neurons (Nakayama et al. 1998). The neurodevelopmental role of FZD9, a third gene found in the critical WS deletion, is of particular interest. FZD9 is expressed most strongly during neuronal migration and appears to be involved in brain growth along the anterior/posterior axis (Wang et al. 1997, 1999). FZD9 is part of the Wnt gene family, which encodes for secreted signaling glycoproteins and are known to be involved in controlling early cell development, tissue differentiation, segmentation, and dorsal–ventral polarity (Cadigan and Nusse 1997). As WS abnormalities tend to be located in dorsal regions (Galaburda and Bellugi 2000), hemizygosity for FZD9 is a potential cause of the global neuroanatomic dysmorphology seen in WS.

Although this study employs highly reliable computer-based technology to reveal new information on WS neuromorphology, it has several limitations. First, the present methodology cannot necessarily distinguish polymicrogyri from larger, deeper gyri as long as the ratio of inner to outer brain contour is identical in both cases. This is somewhat problematic as it is unclear whether increases in gyrification in WS are truly due to a tendency toward polymicrogyri, or simply to differential cortical atrophy. Our laboratories are presently investigating improved methods to distinguish between these two cases. Additionally, although this study describes increased GI, it provides no explanation about the origins of this effect. Further research is needed to correlate alterations in brain morphology with variations in cognitive ability and genotype. These investigations are currently underway.

Accepted for publication 16th November 2001.

Acknowledgements
This research was supported by NIH grants HD33113 to UB at the Salk Institute and MH01142 and HD31715 to AR. This work was also partially supported by a grants from the Packard Foundation, and the Sinclair Fund to AR. We are grateful to the participants in these studies and to the local, regional, and national Williams Syndrome Associations. Special thanks to Julie Korenberg, Zona Lai, and Wendy Jones for their help in the production of the manuscript.

References

Aylward EH, Reiss A. (1991) Area and volume measurement of posterior fossa structures in MRI. *Journal of Psychiatric Research* **25:** 159–68.

Bartley AJ, Jones DW, Weinberger DR. (1997) Genetic variability of human brain size and cortical gyral patterns. *Brain* **120** (**Pt 2**)**:** 257–69.

Bellugi U, Lichtenberger L, Mills D, Galaburda A, Korenberg JR. (1999) Bridging cognition, the brain, and molecular genetics: evidence from Williams syndrome. *Trends in Neuroscience* **22:** 197–207.

Bellugi U, Lichtenberger L, Jones W, Lai Z, St George M. (2000) The neurocognitive profile of Williams Syndrome I: a complex pattern of strengths and weaknesses. *Journal of Cognitive Neuroscience* **12** (Suppl. 1)**:** 7–29.

Cadigan KM, Nusse R. (1997) Wnt signaling: a common theme in animal development. *Genes and Development* **11:** 3286–305.

Dobbing J, Sands J. (1970) Growth and development of the brain and spinal cord of the guinea-pig. *Brain Research* **17:** 115–23.

Galaburda AM, Wang PP, Bellugi U, Rossen M. (1994) Cytoarchitectonic anomalies in a genetically based disorder: Williams syndrome. *Neuroreport* **5:** 753–7.

Galaburda AM, Bellugi U. (2000) V. Multi-level analysis of cortical neuroanatomy in Williams syndrome. *Journal of Cognitive Neuroscience* **12** (Suppl. 1)**:** 74–88.

Korenberg JR, Chen XN, Hirota H, Lai Z, Bellugi U, Burian D, Roe B, Matsuoka R. (2000) VI. Genome structure and cognitive map of Williams syndrome. *Journal of Cognitive Neuroscience* **12** (Suppl. 1)**:** 89–107.

Kulynych JJ, Luevano LF, Jones DW, Weinberger DR. (1997) Cortical abnormality in schizophrenia: an in vivo application of the gyrification index. *Biological Psychiatry* **41:** 995–9.

Lancaster JL, Fox PT, Downs H, Nickerson DS, Hander TA, El Mallah M, Kochunov PV, Zamarripa F. (1999) Global spatial normalization of human brain using convex hulls. *Journal of Nuclear Medicine* **40:** 942–55.

Magnotta VA, Andreasen NC, Schultz SK, Harris G, Cizadlo T, Heckel D, Nopoulos PFlaum M. (1999) Quantitative in vivo measurement of gyrification in the human brain: changes associated with aging. *Cerebral Cortex* **9:** 151–60.

Morris CA, Demsey SA, Leonard CO, Dilts C, Blackburn BL. (1988) Natural history of Williams syndrome: physical characteristics. *Journal of Pediatrics* **113:** 318–26.

Nakayama T, Matsuoka R, Kimura M, Hirota H, Mikoshiba K, Shimizu Y, Shimizu N, Akagawa K. (1998) Hemizygous deletion of the HPC-1/syntaxin 1A gene (STX1A) in patients with Williams syndrome. *Cytogenetics and Cell Genetics* **82:** 49–51.

Ono M, Kubic S, Abernathy C. (1990) *Atlas of the Cerebral Sulci*. New York: Thieme Medical Publishers.

Otsu N. (1979) A threshold selection method from gray-level histograms. *IEEE Transactions on Systems, Man, and Cybernetics* **9:** 62–6.

Rakic P. (1988) *Neurobiology of Neocortex*. Berlin: Chichester & Wiley.

Reiss A. (2000) *BrainImage*. Stanford, CA: Stanford University.

Reiss AL, Eliez S, Schmitt JE, Straus E, Lai Z, Jones W, Bellugi U. (2000) IV. Neuroanatomy of Williams syndrome: a high-resolution MRI study. *Journal of Cognitive Neuroscience* **12** (Suppl. 1)**:** 65–73.

Richman DP, Stewart RM, Hutchinson JW, Caviness VS Jr. (1975) Mechanical model of brain convolutional development. *Science* **189:** 18–21.

Schmitt JE, Eliez S, Bellugi U, Reiss AL. (2001) Analysis of cerebral shape in Williams Syndrome. *Archives of Neurology* **58:** 283–7.

Schmitt JE, Eliez S, Warsofsky IS, Bellugi U, Reiss AL. (2001) Corpus callosum morphology in Williams syndrome: relation to genetics and behavior. *Developmental Medicine & Child Neurology* **43:** 155–59.

Subramaniam B, Hennessey JG, Rubin MA, Beach LS, Reiss AL. (1997) Software and methods for quantitative imaging in neuroscience: the Kennedy Krieger Institute Human Brain Project. In: Koslow SH, Huerta MF, editors. *Neuroinformatics: An Overview of the Human Brain Project*. Mahwah, NJ: Lawrence Erlbaum.

Talairach J, Tournoux P. (1988) *Co-planar Stereotaxic Atlas of the Human Brain*. New York: Thieme Medical Publishers.

Todd PH. (1982) A geometric model for the cortical folding pattern of simple folded brains. *Journal of Theoretical Biology* **97:** 529–38.

Trauner DA, Bellugi U, Chase C. (1989) Neurologic features of Williams and Down syndromes. *Pediatric Neurology* **5:** 166–8.

Van Essen DC, Maunsell JH. (1980) Two-dimensional maps of the cerebral cortex. *Journal of Comparative Neurology* **191:** 255–81.

Vogeley K, Schneider-Axmann T, Pfeiffer U, Tepest R, Bayer TA, Bogerts B, Honer WG, Falkai P. (2000) Disturbed gyrification of the prefrontal region in male schizophrenic patients: a morphometric post-mortem study. *American Journal of Psychiatry* **157:** 34–9.

Wang JY, Frenzel KE, Wen D, Falls DL. (1998) Transmembrane neuregulins interact with LIM kinase 1, a cytoplasmic protein kinase implicated in development of visuospatial cognition. *Journal of Biological Chemistry* **273:** 20525–34.

Wang YK, Samos CH, Peoples R, Perez-Jurado LA, Nusse R, Francke U. (1997) A novel human homologue of the Drosophila frizzled wnt receptor gene binds wingless protein and is in the Williams syndrome deletion at 7q11.23. *Human Molecular Genetics* **6:** 465–72.

Wang YK, Sporle R, Paperna T, Schughart K, Francke U. (1999) Characterization and expression pattern of the frizzled gene Fzd9, the mouse homolog of FZD9 which is deleted in Williams-Beuren syndrome. *Genomics* **57:** 235–48.

Zilles K, Armstrong E, Schleicher A, Kretschmann HJ. (1988) The human pattern of gyrification in the cerebral cortex. *Anatomy and Embryology* **179:** 173–9.